

## † Electronic Supporting Information

### Quaternary ammonium bearing hyper-crosslinked polymer encapsulation on Fe<sub>3</sub>O<sub>4</sub> nanoparticles

Prakash B. Rathod,<sup>a,b</sup> Ashok K. Pandey,<sup>a\*</sup> Sher Singh Meena<sup>c</sup> and Anjali  
A. Athawale<sup>b\*</sup>

---

<sup>a</sup> Radiochemistry Division, Bhabha Atomic Research Centre, Trombay, Mumbai 400 085, India; and Homi Bhabha National Institute, Anushaktinagar, Mumbai 400 094, India. Fax: +91-22-25505151; Tel: +91-22-25594566; E-mail: [ashokk@barc.gov.in](mailto:ashokk@barc.gov.in), [memgreek@gmail.com](mailto:memgreek@gmail.com).

<sup>b</sup> Department of Chemistry, Savitribai Phule Pune University, Pune-411 007, India; E-mail: [agbed@chem.unipune.ac.in](mailto:agbed@chem.unipune.ac.in)

<sup>c</sup> Solid State Physics Division, Bhabha Atomic Research Centre, Trombay, Mumbai 400 085, India. E-mail: [ssingh@barc.gov.in](mailto:ssingh@barc.gov.in).

**Fig. S1** Rietveld refined X-ray diffraction patterns of  $\text{Fe}_3\text{O}_4$  particles prepared by co-precipitation method using  $\text{Fe}^{2+}$  salt (a) and 1:2 mol proportions of  $\text{Fe}^{2+}$  and  $\text{Fe}^{3+}$  salts (b).

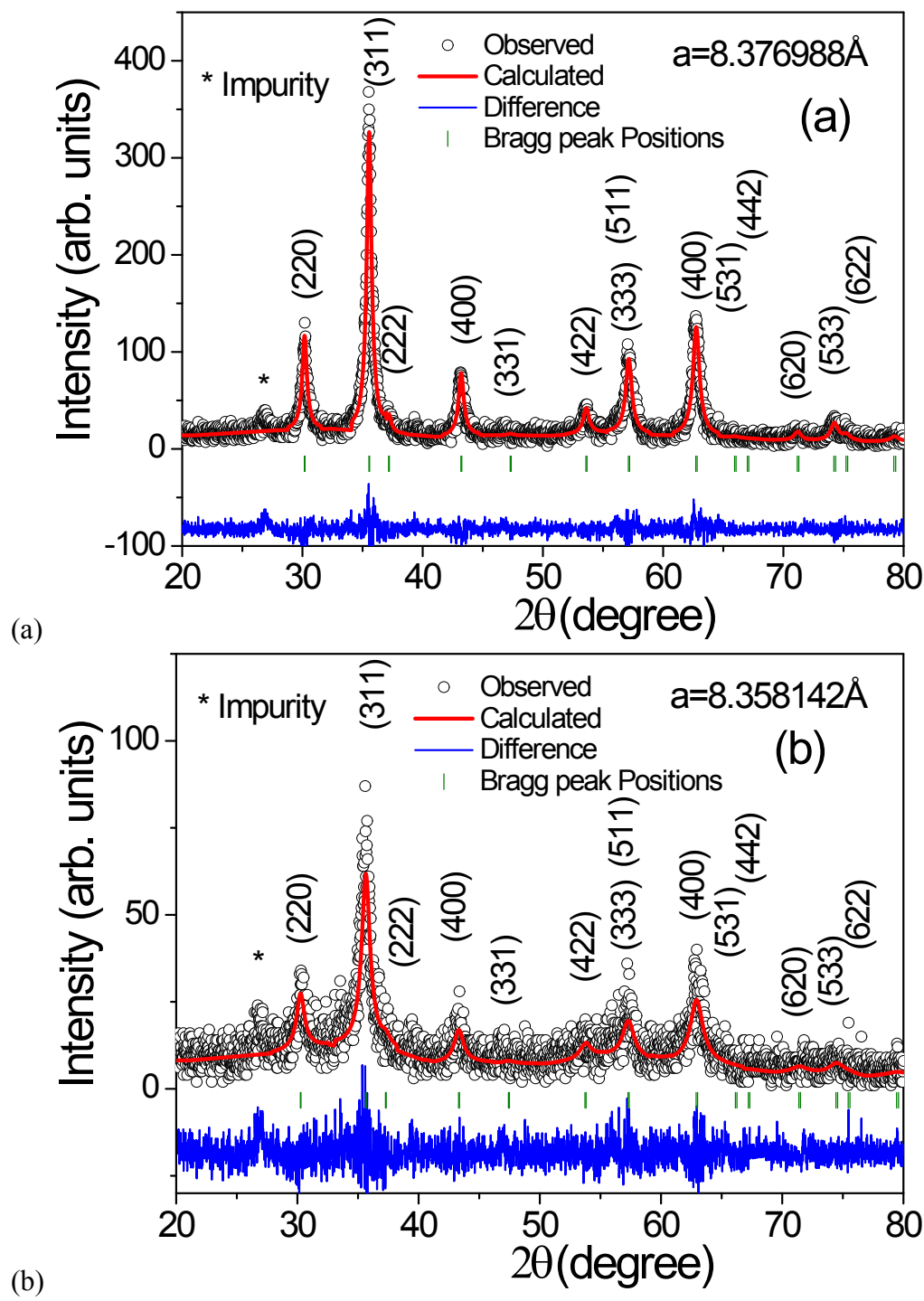


**Fig. S2** VSM magnetization curves for the Fe<sub>3</sub>O<sub>4</sub> particles (MNP) coated with TEOS, TEOS+APTES, and APTES.

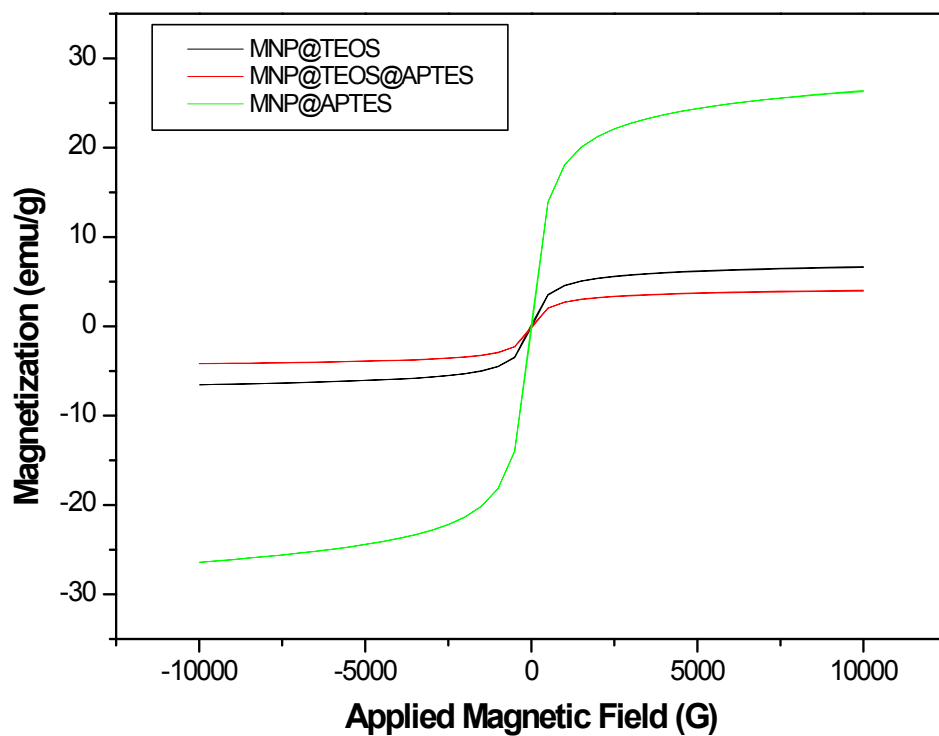
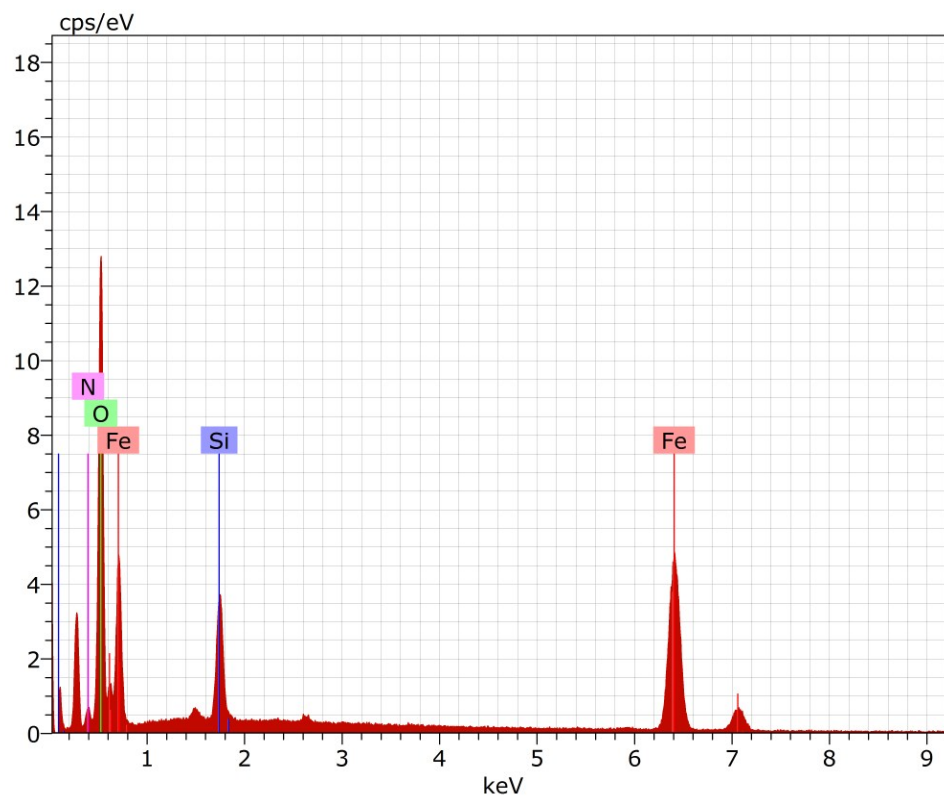


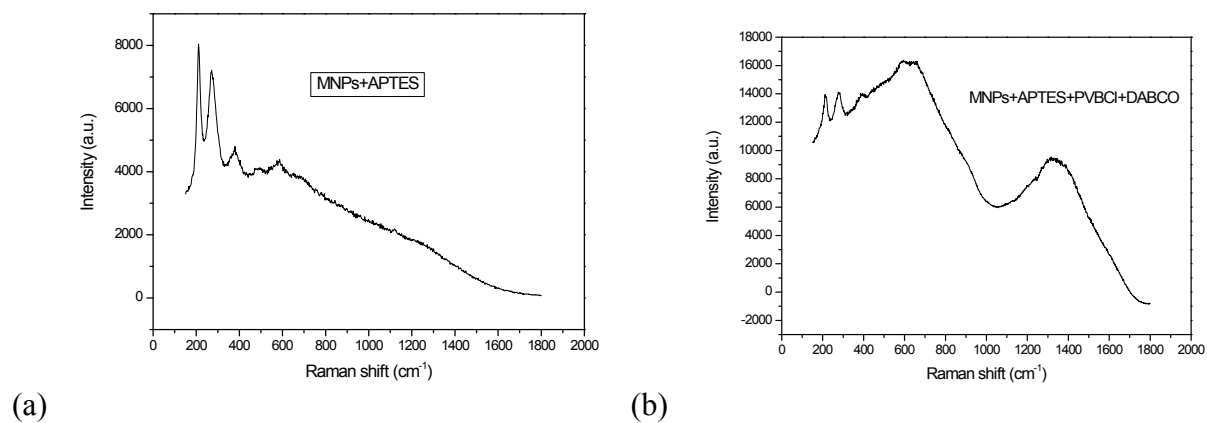
**Fig. S3** EDS spectrum of Fe<sub>3</sub>O<sub>4</sub>@PVB-DABCO-DBO showing the presence of expected elements.



Spectrum: A 282

El	AN	Series	unn. C [wt.%]	norm. C [wt.%]	Atom. C [at.%]	Error (1 Sigma) [wt.%]
Fe	26	K-series	51.36	48.42	20.25	1.55
O	8	K-series	32.19	30.35	44.29	3.81
C	6	K-series	14.75	13.91	27.04	2.06
Si	14	K-series	4.80	4.52	3.76	0.23
N	7	K-series	2.97	2.80	4.67	0.59
Total:			106.07	100.00	100.00	

**Fig. S4** Raman spectra of APTS coated  $\text{Fe}_3\text{O}_4$  (a) and  $\text{Fe}_3\text{O}_4@\text{PVB-DABCO-DBO}$  (b) particles.

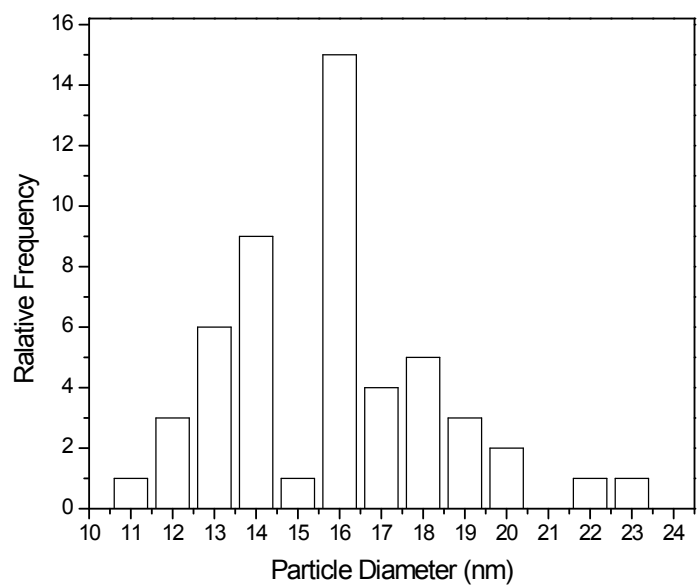


Silane:-  $500\text{-}520\text{ cm}^{-1}$

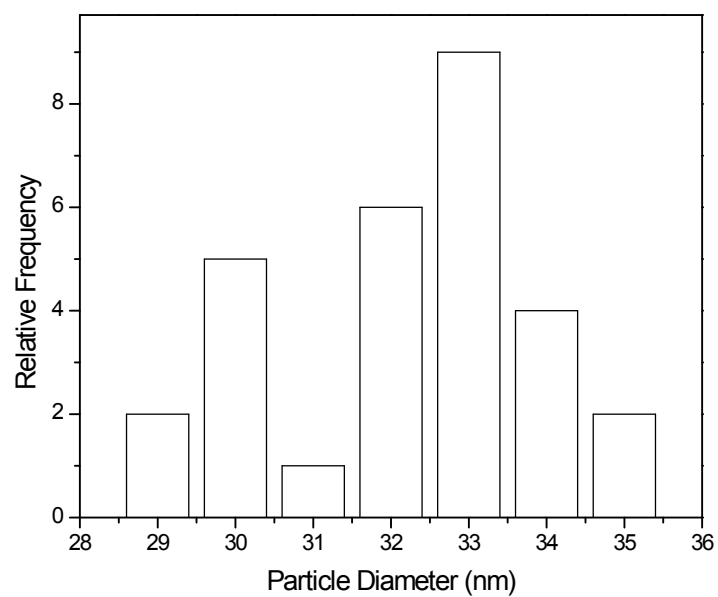
MNPS:- Peak between  $200\text{-}500\text{ cm}^{-1}$

Rest peaks are aliphatic chain and aromatic chain ring vibrations.

**Fig. S5** Histograms of size distributions of pristine  $\text{Fe}_3\text{O}_4$  particles (a) and  $\text{Fe}_3\text{O}_4@\text{PVB-DABCO-DBO}$  (b) obtained from the FE-SEM images.



(a)



(b)

### (c) DATA ANALYSES SECTION

#### XRD Analysis

The average crystallite size ( $D_{XRD}$ ) of the nano phase particles were determined by using the Debye-Scherer formula

$$D_{XRD} = \frac{K\lambda}{\beta \cos \theta}$$

Where  $K$  is the Scherrer's constant (shape factor  $K=0.9$ , assumes spherical crystallites),  $\lambda$  is the wavelength of the Cu  $K_{\alpha}$  radiation ( $\lambda= 1.541874 \text{ \AA}$ ) and  $\beta$  is the full width at half maximum (FWHM) in radians calculated using Gaussian fitting and  $\theta$  denotes the Bragg angle. The average crystallite sizes for both the samples are given in Table 1. It is observed that the lattice constant decreases with decreasing crystallite size.<sup>1</sup> The crystallite size calculated by using three most intense peaks (220, 311 and 400).

<b>Table S1.</b> Crystallite size and Lattice constants of Fe <sub>3</sub> O <sub>4</sub> particles prepared by co-precipitation method.		
<b>Sample</b>	<b>Average Crystallite size <math>D_{XRD}</math> (nm)</b>	<b>Lattice constant (<math>a_r</math>) (<math>\text{\AA}</math>)</b>
Using single ferrous salt	25	8.376988
Using ferrous + ferric salts	13	8.358142

## Mössbauer Studies

**Table S2.** The Hyperfine magnetic field ( $H_{\text{hf}}$ ), isomer shift ( $\delta$ ), quadrupole splitting ( $\Delta$ ), linewidth ( $\Gamma$ ) and relative intensity (RI) in percentage of tetrahedral and octahedral sites of  $\text{Fe}^{3+}/\text{Fe}^{2+}$  ions for  $\text{Fe}_3\text{O}_4$  ferrite MNPs derived from Mössbauer spectra recorded at room temperature. Isomer shift values are relative to Fe metal foil ( $\delta = 0.0$  mm/s). Sextet A: Tetrahedral site ( $\text{Fe}^{3+}$ ), Sextet B: Octahedral site ( $\text{Fe}^{3+}$  and  $\text{Fe}^{2+}$ ), C: ( $\text{Fe}^{3+}$ ), Doublet: ( $\text{Fe}^{3+}$ ).

$\text{Fe}_3\text{O}_4$	Iron sites	Relative area ( $R_A$ ) %	Inner line width, ( $\Gamma$ ) mm/s	Isomer shift, ( $\delta$ ) mm/s	Quadrupole splitting, ( $\Delta$ ) mm/s	Hyperfine field ( $H_{\text{hf}}$ ) Tesla	Fitting quality ( $\chi^2$ )
Sample-1	Doublet	3.82	0.435	0.358	0.680	--	1.9094
	Sextet A	15.57	0.384	0.295	-0.023	48.91	
	Sextet B	24.69	0.728	0.463	-0.029	45.30	
	Sextet C	55.92	1.91	0.375	0.036	39.08	
Sample-2	Doublet	33.92	0.497	0.372	0.666	--	1.1645
	Sextet A	13.21	0.500	0.192	-0.045	46.97	
	Sextet B	17.01	1.208	0.618	0.179	46.04	
	Sextet C	35.84	1.135	0.482	0.003	40.18	

The value of  $\delta_A < \delta_B$ ,<sup>2-7</sup> and  $H_{\text{hf}}$  are higher for tetrahedral site than that of the octahedral site in  $\text{Fe}_3\text{O}_4$  ferrite.<sup>8-9</sup> The value of the quadrupole splitting was almost zero for sextets for sample-1 indicating the cubic crystal structure.<sup>10</sup> The detailed analyses of Mössbauer spectra are given in the supporting information. Mössbauer spectra of both samples show a paramagnetic doublet with  $\delta$ ,  $\Delta$ ,  $\Gamma$  and  $R_A$  values as  $\delta = 0.358$  and  $0.372$  mm/s,  $\Delta = 0.680$  and  $0.666$  mm/s,  $\Gamma = 0.435$  and  $0.497$  mm/s,  $R_A = 3.82$  and  $33.92$  %, respectively. These values are indicating the presence of  $\text{Fe}^{3+}$  ions in high spin state and situated in distorted local lattice environments. The value of quadrupole splitting of the doublet is larger than that of the sextets. It is because the particle sizes represented by the doublet are small and their magnetic structure is not complete. These signify



more crystal defects and lattice distortions, which result in reducing the symmetry around the Fe ions. The relative percentage of sextet to doublet patterns for the samples a and b are found to be 96.18:3.82 and 76.08: 33.92, respectively, indicating that the superparamagnetic fraction is small in sample a.

According to the theory of superparamagnetic blocking temperature ( $T_B$ ) for nanometer size particles, the  $T_B$  is directly proportional to particle volume ( $V$ ) and can be represented as  $T_B = KV/25k_B$ , where  $K$  is the anisotropy energy density constant and  $k_B$  is the Boltzmann's constant. The nanosized magnetic particles are single domain particles and they become superparamagnetic below a critical size ( $d_c$ ) and above the blocking temperature ( $T_B$ ). i.e. magnetization direction fluctuates spontaneously (superparamagnetic relaxation) with a relaxation time ( $\tau$ ). When  $\tau$  is less than or equal to  $10^{-9}$  s, it results in the disappearance of the magnetic splitting to show the superparamagnetic doublet,<sup>10-11</sup> as observed in the Mössbauer spectra for both the samples (Figure 2). The relative areas of the nanosized particles of the samples a and b are 3.8 and 33.9 %, respectively when their  $T_B$  is below the room temperature. The value of line width of sextet A and B is higher for sample (b) due to the comparatively lower particle size. It is also further confirmed from the hyperfine magnetic field of tetrahedral A site (sextet A). The value of  $H_{hf}$  is found to be reduced for tetrahedral A of sample (b). The value of  $H_{hf}$  is observed to decrease with decrease in particle size as observed in the Mössbauer spectrum.<sup>11</sup> When the particle size decreases the value of  $H_{hf}$  will be reducing. It is also confirmed from the room temperature XRD data that the sample-b is having smaller particle size compared to sample-a.

## References

1. Dependence of Lattice Parameter on Particle Size, S A Nepijco, E. Pippel, J. woltersdorf, Phys. Stat. Sol. (a) 61 469 (1980).
2. N. N. Greenwood and T. C. Gibb, Mössbauer Spectroscopy (*Chapman and Hall Ltd., London, 1971*).
3. K. Sharma, Sher Singh Meena, C. L. Prajapat, S. Bhattacharya, Jagannath, M. R. Singh, S. M. Yusuf, G. P. Kothiyal, J. Magn. Mater. 321 (2009) 3821.
4. K. Sharma, A. Dixit, Sher Singh, Jagannath, S. Bhattacharya, C.L. Prajapat, P.K. Sharma, S.M. Yusuf, A. K. Tyagi, G.P. Kothiyal, Mater. Sci. Eng. C 29 (2009) 2226.
5. K. Sharma, Sher Singh Meena, Sudhanshu Saxena, S.M. Yusuf, A. Srinivasan, G. P. Kothiyal, Mater. Chem. Phys. 133 (2012) 144.
6. S. S. Shinde, Sher Singh Meena, S. M. Yusuf, and K. Y. Rajpure, J. Phys. Chem. C 2011, 115, 3731–3736.

7. S. C. Bhargava, A. H. Morrish, H. Kunkel, and Z. W. Li, *J. Phys.: Condens. Matter* 12 (2000) 9667-9687.
8. Goya, G. F.; Berquo, T. S.; Fonseca, F. C.; Morales, M. P. Static and Dynamic Magnetic Properties of Spherical Magnetite Nanoparticles, *J. Appl. Phys.* 2003, 94, 3520–3528.
9. Santoyo Salazar, J.; Perez, L.; de Abril, O.; Truong Phuoc, L.; Ihiwakrim, D.; Vazquez, M.; Greneche, J.-M.; Begin-Colin, S.; Pourroy, G. Magnetic Iron Oxide Nanoparticles in 10–40 nm Range: Composition in Terms of Magnetite/Maghemite Ratio and Effect on the Magnetic Properties. *Chem. Mater.* 2011, 23, 1379–1386.
10. Ghosh, R.; Pradhan, L.; Devi, Y. P.; Meena, S. S.; Tewari, R.; Kumar, A.; Sharma, S.; Gajbhiye, N. S.; Vatsa, R. K.; Pandey, B. N.; Ningthoujam, R. S. Induction Heating Studies of  $\text{Fe}_3\text{O}_4$  Magnetic Nanoparticles Capped with Oleic Acid and Polyethylene Glycol for Hyperthermia. *J. Mater. Chem.* 2011, 21, 13388–13398.
11. K. Vasundhara, S. N. Achary, S. K. Deshpande, P. D. Babu, S. S. Meena, and A. K. Tyagi, Size dependent magnetic and dielectric properties of nano  $\text{CoFe}_2\text{O}_4$  prepared by a salt assisted gel-combustion method, *J. Appl. Phys.* 113, 194101 (2013).